

On Multipolar Analytical Potentials for Galaxies

Daniel Vogt*

Instituto de Física Gleb Wataghin, Universidade Estadual de Campinas
13083-970 Campinas, S. P., Brazil

Patricio S. Letelier†

Departamento de Matemática Aplicada-IMECC, Universidade Estadual
de Campinas 13083-970 Campinas, S. P., Brazil

December 16, 2018

Abstract

We present analytical potential–density pairs in three dimensions for the gravitational field of galaxies, obtained by thickening the multipolar expansion up to the quadrupole term. These may be interpreted as generalizations of the Miyamoto and Nagai potential–density pairs. With a suitable restriction on the possible values of the multipole moments, the density distributions are positive and monotone decreasing functions of the radial and axial coordinates.

Key Words: galaxies: kinematics and dynamics – galaxies: structure

1 Introduction

There are several three-dimensional analytical models in the literature for the gravitational field of different types of galaxies and galactic components. Jaffe (1983) and Hernquist (1990) discuss models for spherical galaxies and bulges. Three-dimensional models for flat galaxies were obtained by Miyamoto and Nagai (1975) and Satoh (1980). de Zeeuw and Pfenniger (1989) considered a set of ellipsoidal models appropriate to galactic bars. Long and Murali (1992) derived simple potential–density pairs for a prolate and a triaxial bar by softening a thin needle with a spherical and

*e-mail: danielvt@ifc.unicamp.br

†e-mail: letelier@ime.unicamp.br

a Miyamoto and Nagai potential, respectively. See Binney and Tremaine (1987) for a discussion of other galactic models. There also exist several general relativistic models of disks, e.g., Morgan and Morgan (1969, 1970), Bičák et al. (1993), Lemos and Letelier (1994), González and Letelier (2000, 2004), Vogt and Letelier (2003, 2005a). Recently, a general relativistic version of the Miyamoto and Nagai models was studied (Vogt and Letelier 2005b).

The potential–density pairs obtained by Miyamoto and Nagai (1975) are inflated versions of the thin-disk family first derived by Toomre (1963). In this work we consider a set of three-dimensional potential–density pairs obtained by using the same procedure of Miyamoto and Nagai on the multipolar expansion up to the quadrupole term. This generates a sequence of potential–density pairs that reduces to that of Miyamoto and Nagai for particular values of the multipole moments. This is done in subsection 2.1 and subsection 2.2. The thin-disk limit is investigated in subsection 2.3 and corresponds to generalizations of Toomre’s family of disks. Finally, the results are discussed in section 3.

2 Multipolar Models for Flattened Galaxies

A general expression for a multipolar expansion in spherical coordinates can be cast as

$$\Phi = - \sum_{n=0}^{\infty} a_n \frac{P_n(\cos \theta)}{r^{n+1}}, \quad (1)$$

where P_n are the Legendre polynomials and a_n are coefficients related to the multipolar moments. We consider only the expansion up to the quadrupole term ($n = 2$). In cylindrical coordinates the explicit form reads

$$\Phi = - \frac{Gm}{\sqrt{R^2 + z^2}} - \frac{Dz}{(R^2 + z^2)^{3/2}} - \frac{Q(-R^2 + 2z^2)}{2(R^2 + z^2)^{5/2}}, \quad (2)$$

where D and Q are the dipole and quadrupole moments, respectively.

In the following three-dimensional models the mass-density distribution is obtained directly from Poisson equation,

$$\rho = \frac{1}{4\pi G} \left(\Phi_{,RR} + \frac{\Phi_{,R}}{R} + \Phi_{,zz} \right). \quad (3)$$

Other physical quantities of interest are the circular velocity, v_c of particles in the galactic plane, the epicyclic frequency, κ , and the vertical frequency,

ν , of small oscillations about the equilibrium circular orbit in the galactic plane. They are calculated with the expressions (Binney and Tremaine 1987):

$$v_c^2 = R\Phi_{,R}, \quad (4)$$

$$\kappa^2 = \Phi_{,RR} + \frac{3}{R}\Phi_{,R}, \quad (5)$$

$$\nu^2 = \Phi_{,zz}, \quad (6)$$

where all quantities are evaluated on $z = 0$. The stability conditions are set by $\kappa^2 \geq 0$ and $\nu^2 \geq 0$.

2.1 Generalized Miyamoto and Nagai Model 2

We first consider $Q = 0$, and apply the transformation $z \rightarrow a + \sqrt{z^2 + b^2}$ on the multipolar expansion equation (2), where a, b are non-negative constants. Using equation (3), we obtain

$$\tilde{\rho} = \frac{\tilde{b}^2}{4\pi\xi^3 [\tilde{R}^2 + (1 + \xi)^2]^{7/2}} \left\{ \tilde{R}^4(1 - \tilde{D}) + \tilde{R}^2(1 + \xi) \left[\tilde{D}(1 - 8\xi) \right. \right. \\ \left. \left. + (1 + \xi)(2 + 3\xi) \right] + (1 + \xi)^3 \left[2\tilde{D}(1 + 4\xi) + (1 + \xi)(1 + 3\xi) \right] \right\}, \quad (7)$$

where the variables and parameters were rescaled in terms of a : $\tilde{R} = R/a$, $\tilde{z} = z/a$, $\tilde{b} = b/a$, $\tilde{D} = D/(Gma)$, $\rho = m\tilde{\rho}/a^3$, and $\xi = \sqrt{\tilde{z}^2 + \tilde{b}^2}$. For the particular value $\tilde{D} = 1$, equation (7) reduces to the mass density of the Miyamoto–Nagai model 2.

Unfortunately the density distribution, equation (7), has some defects. For certain ranges of the parameters \tilde{b} and \tilde{D} it is not a monotone decreasing function of the radial and axial coordinates, and even has domains with negative densities. To overcome this, we impose a reasonable restriction that the derivative of the density distribution with respect to the \tilde{R} coordinate along $\tilde{z} = 0$ should have only one critical point at $(\tilde{R}, \tilde{z}) = (0, 0)$ as well as the derivative with respect to \tilde{z} along $\tilde{R} = 0$. A graphical study of the resulting equations is displayed in figures 1a–b. In figure 1a the curves of $\tilde{\rho}_{,\tilde{R}} = 0$ are plotted as functions of the radial coordinate and the parameter \tilde{D} for some values of \tilde{b} . In this case decreasing \tilde{b} narrows the interval of \tilde{D} for which there are no other critical points, as on $\tilde{R} = 0$. Figure 1b shows the curve of $\tilde{\rho}_{,\tilde{z}} = 0$ as functions of \tilde{z} and \tilde{D} for the same values of \tilde{b} . One can see from both graphs that the allowed interval for the parameter \tilde{D} for

a fixed value of \tilde{b} in the case (a) is contained in the allowed interval in case (b).

The expressions for the circular velocity, epicyclic frequency and vertical frequency follow from equations (4)–(6)

$$\tilde{v}_c^2 = \frac{\tilde{R}^2 \left[\tilde{R}^2 + (1 + \tilde{b})(1 + \tilde{b} + 3\tilde{D}) \right]}{\left[\tilde{R}^2 + (1 + \tilde{b})^2 \right]^{5/2}}, \quad (8)$$

$$\tilde{\kappa}^2 = \frac{1}{\left[\tilde{R}^2 + (1 + \tilde{b})^2 \right]^{7/2}} \left\{ \tilde{R}^4 + \tilde{R}^2(1 + \tilde{b}) \left[5(1 + \tilde{b}) - 3\tilde{D} \right] + 4(1 + \tilde{b})^3(1 + \tilde{b} + 3\tilde{D}) \right\}, \quad (9)$$

$$\tilde{\nu}^2 = \frac{\tilde{R}^2(1 + \tilde{b} - \tilde{D}) + (1 + \tilde{b})^2(1 + \tilde{b} + 2\tilde{D})}{\tilde{b} \left[\tilde{R}^2 + (1 + \tilde{b})^2 \right]^{5/2}}, \quad (10)$$

where $v_c^2 = Gm\tilde{v}_c^2/a$, $\kappa^2 = Gm\tilde{\kappa}^2/a^3$, and $\nu^2 = Gm\tilde{\nu}^2/a^3$. The condition $\tilde{v}_c^2 \geq 0$ and the stability conditions $\kappa^2 \geq 0$ and $\nu^2 \geq 0$ also impose restrictions on the possible values of \tilde{D} and \tilde{b} . We find that $\tilde{D} \geq -(1 + \tilde{b})/3$ ensures the positivity of the circular velocity and of the square of the epicyclic frequency, whereas the square of the vertical frequency is always non-negative if $\tilde{D} \geq -(1 + \tilde{b})/2$.

In figures 2a–c we plot some isodensity curves of the density function, equation (7), with parameter $\tilde{b} = 0.5$ and (a) $\tilde{D} = 1$, (b) $\tilde{D} = 0.5$, and (c) $\tilde{D} = -0.1$. For these values the density is a monotone decreasing function, as can be checked from figure 1. It is clearly seen that as the parameter \tilde{D} decreases, the density distribution becomes more flattened. Figure 2d and figures 3a–b show, respectively, curves of the velocity profile, equation (8), the epicyclic frequency, equation (9), and of the vertical frequency, equation (10), for the same parameters as in figures 2a–c. With decreasing \tilde{D} the radius where the highest circular velocity occurs is increased and the epicyclic frequency is lowered. The vertical frequency becomes lower near the center, but for $\tilde{R} \gtrsim 2$ it is increased.

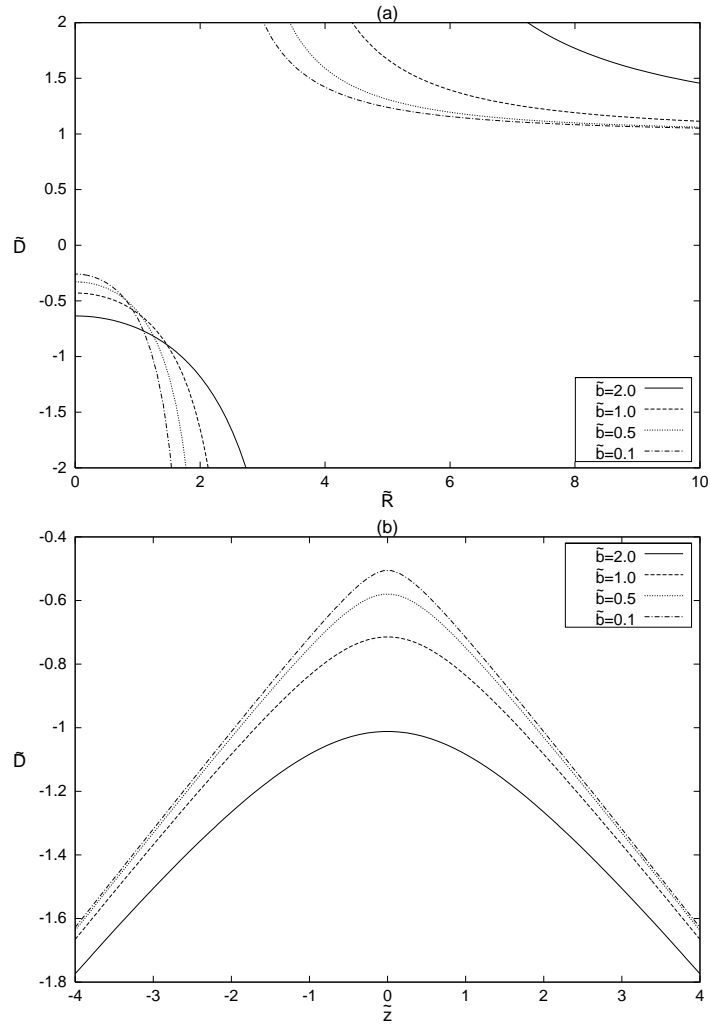


Figure 1: (a) Curves of $\tilde{\rho}_{,\tilde{R}} = 0$ as functions of \tilde{R} and \tilde{D} for $\tilde{b} = 2, 1, 0.5,$ and 0.1 . (b) $\tilde{\rho}_{,\tilde{z}} = 0$ as functions of \tilde{z} and \tilde{D} for $\tilde{b} = 2, 1, 0.5,$ and 0.1 .

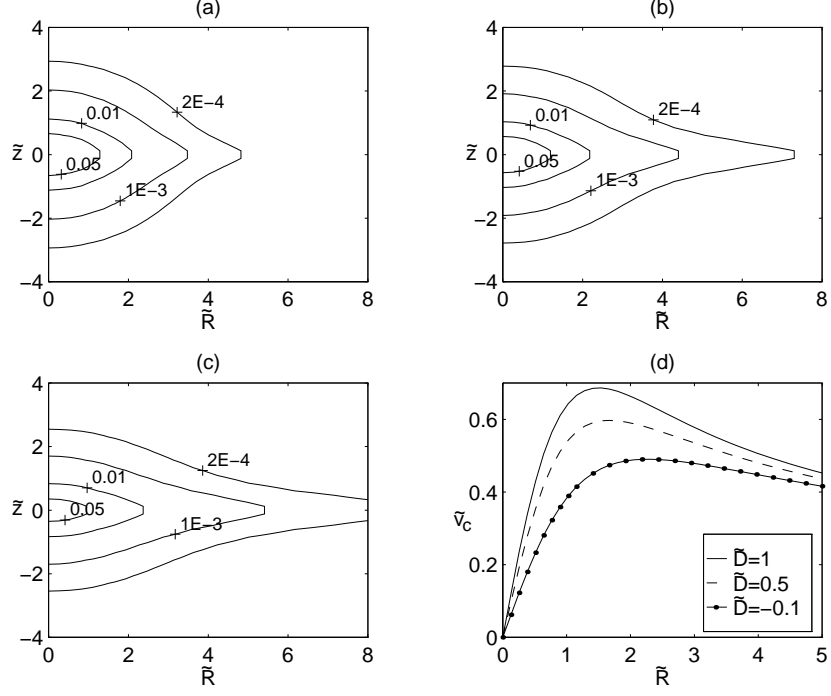


Figure 2: Constant-density curves of equation (7) with parameters $\tilde{b} = 0.5$ and (a) $\tilde{D} = 1$, (b) $\tilde{D} = 0.5$, and (c) $\tilde{D} = -0.1$. (d) The circular velocity \tilde{v}_c (equation (8)), in the galactic plane for cases (a)–(c).

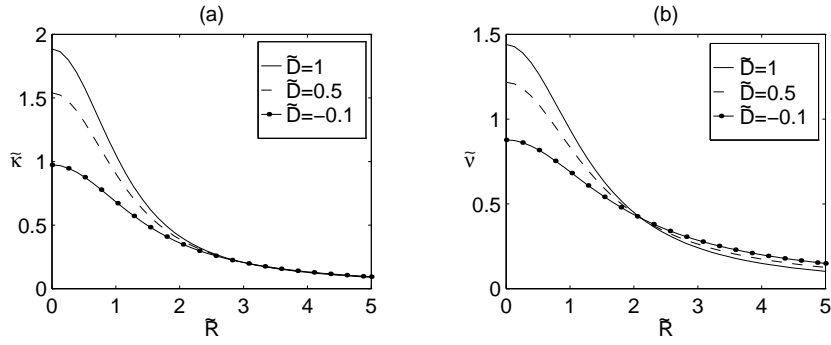


Figure 3: Curves of (a) the epicyclic frequency, $\tilde{\kappa}$ (equation (9)), and (b) the vertical frequency, $\tilde{\nu}$ (equation (10)), for the same parameters as in figure 2.

2.2 Generalized Miyamoto and Nagai Model 3

We now consider the full expression equation (2) and apply the transformation $z \rightarrow a + \sqrt{z^2 + b^2}$. The resulting mass density distribution reads

$$\begin{aligned} \tilde{\rho} = & \frac{\tilde{b}^2}{8\pi\xi^3 [\tilde{R}^2 + (1 + \xi)^2]^{9/2}} \left\{ 2\tilde{R}^6(1 - \tilde{D}) + 3\tilde{R}^4 \left[2(1 + \xi)^3 - 6\tilde{D}\xi(1 + \xi) \right. \right. \\ & \left. \left. - 3\tilde{Q} \right] + 3\tilde{R}^2(1 + \xi)^2 \left[2(1 + \xi)^2(1 + 2\xi) + 2\tilde{D}(1 + \xi) - \tilde{Q}(1 + 25\xi) \right] \right. \\ & \left. + 2(1 + \xi)^4 \left[(1 + \xi)^2(1 + 3\xi) + 2\tilde{D}(1 + \xi)(1 + 4\xi) + 3\tilde{Q}(1 + 5\xi) \right] \right\}, \quad (11) \end{aligned}$$

where the variables and parameters have been rescaled, as in subsection 2.1 and $\tilde{Q} = Q/(Gma^2)$. For particular values $\tilde{D} = 1$, $\tilde{Q} = 2/3$ we recover the Miyamoto and Nagai model 3.

Also here the range of the parameters must be restricted to produce physically acceptable density distributions. In figures 4a–b we show, respectively, some curves of $\tilde{\rho}_{,\tilde{R}} = 0$ along $\tilde{z} = 0$ and $\tilde{\rho}_{,\tilde{z}} = 0$ along $\tilde{R} = 0$ as functions of \tilde{Q} for some sets of values of \tilde{D} and \tilde{b} . The expressions for the circular velocity, epicyclic frequency and vertical frequency follow from equations (4)–(6)

$$\begin{aligned} \tilde{v}_c^2 = & \frac{\tilde{R}^2}{2 [\tilde{R}^2 + (1 + \tilde{b})^2]^{7/2}} \left\{ 2\tilde{R}^4 + \tilde{R}^2 \left[4(1 + \tilde{b})^2 + 6\tilde{D}(1 + \tilde{b}) - 3\tilde{Q} \right] \right. \\ & \left. + 2(1 + \tilde{b})^2 \left[(1 + \tilde{b})^2 + 3\tilde{D}(1 + \tilde{b}) + 6\tilde{Q} \right] \right\}, \quad (12) \end{aligned}$$

$$\begin{aligned} \tilde{\kappa}^2 = & \frac{1}{2 [\tilde{R}^2 + (1 + \tilde{b})^2]^{9/2}} \left\{ 2\tilde{R}^6 + 3\tilde{R}^4 \left[4(1 + \tilde{b})^2 - 2\tilde{D}(1 + \tilde{b}) + \tilde{Q} \right] \right. \\ & + 18\tilde{R}^2(1 + \tilde{b})^2 \left[(1 + \tilde{b})^2 + \tilde{D}(1 + \tilde{b}) - 3\tilde{Q} \right] \\ & \left. + 8(1 + \tilde{b})^4 \left[(1 + \tilde{b})^2 + 3\tilde{D}(1 + \tilde{b}) + 6\tilde{Q} \right] \right\}, \quad (13) \end{aligned}$$

$$\begin{aligned} \tilde{\nu}^2 = & \frac{1}{2\tilde{b} [\tilde{R}^2 + (1 + \tilde{b})^2]^{7/2}} \left\{ 2\tilde{R}^4(1 + \tilde{b} - \tilde{D}) + \tilde{R}^2(1 + \tilde{b}) \left[4(1 + \tilde{b})^2 \right. \right. \\ & \left. \left. + 2\tilde{D}(1 + \tilde{b}) - 9\tilde{Q} \right] + 2(1 + \tilde{b})^3 \left[(1 + \tilde{b})^2 + 2\tilde{D}(1 + \tilde{b}) + 3\tilde{Q} \right] \right\}, \quad (14) \end{aligned}$$

A graphical analysis of the constraints on the parameters imposed by $\tilde{v}_c^2 \geq 0$, $\tilde{\kappa}^2 \geq 0$ and $\tilde{\nu}^2 \geq 0$ shows that they are contained in the restrictions imposed by the gradient of the mass density.

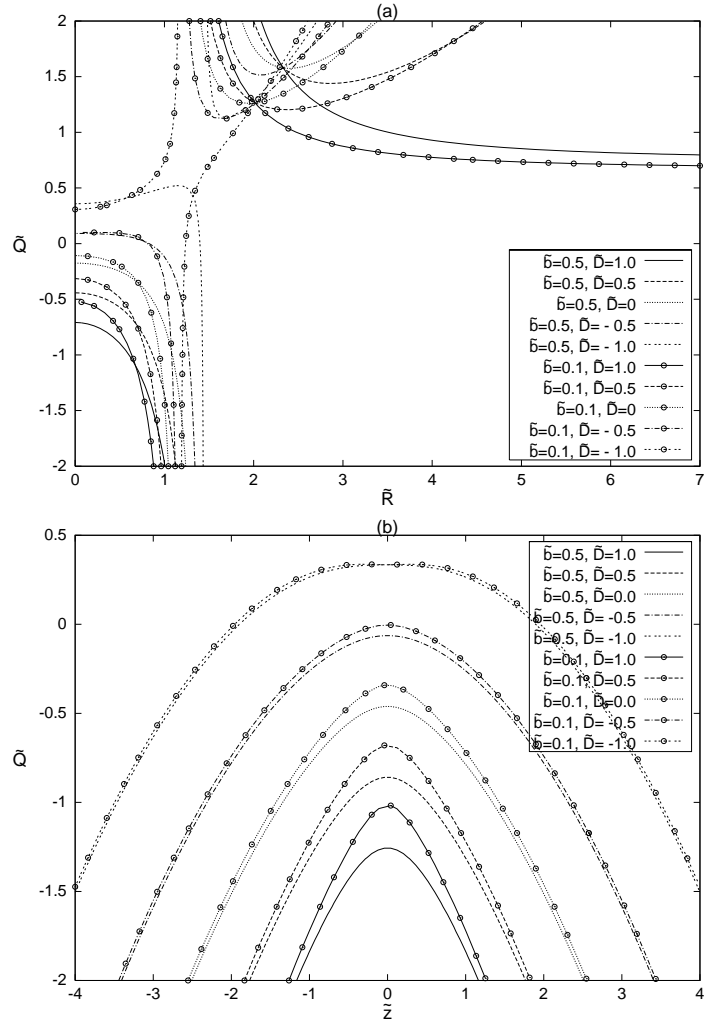


Figure 4: (a) Curves of $\tilde{\rho}_{\tilde{R}} = 0$ as functions of \tilde{R} and \tilde{Q} for some values of the parameters \tilde{b} and \tilde{D} . (b) Curves of $\tilde{\rho}_{\tilde{z}} = 0$ as functions of \tilde{z} and \tilde{Q} for some values of the parameters \tilde{b} and \tilde{D} .

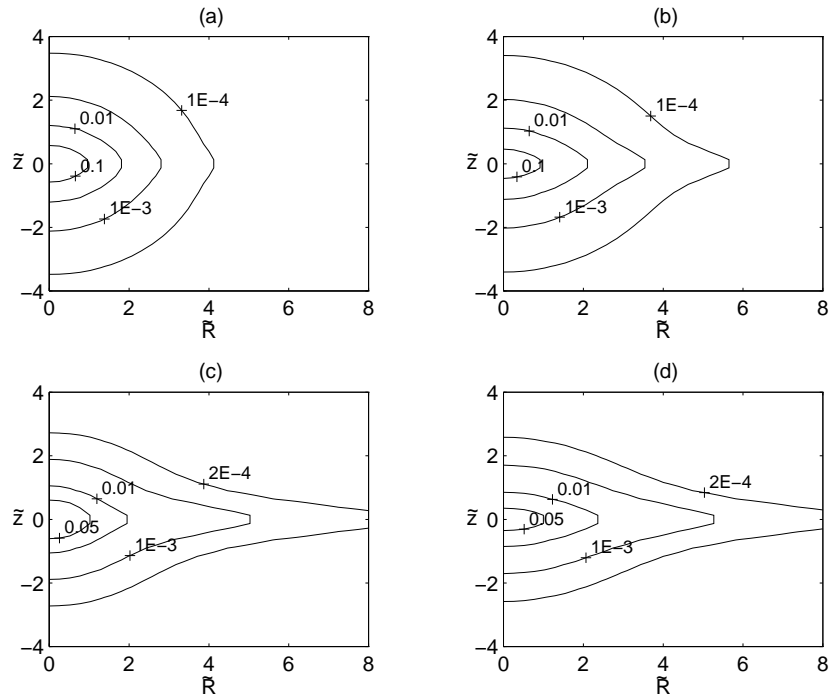


Figure 5: Constant density curves of equation (11) with parameters $\tilde{b} = 0.5$ and (a) $\tilde{D} = 1$, $\tilde{Q} = 2/3$, (b) $\tilde{D} = 1$, $\tilde{Q} = -0.1$, (c) $\tilde{D} = 0$, $\tilde{Q} = 2/3$, and (d) $\tilde{D} = 0$, $\tilde{Q} = -0.1$.

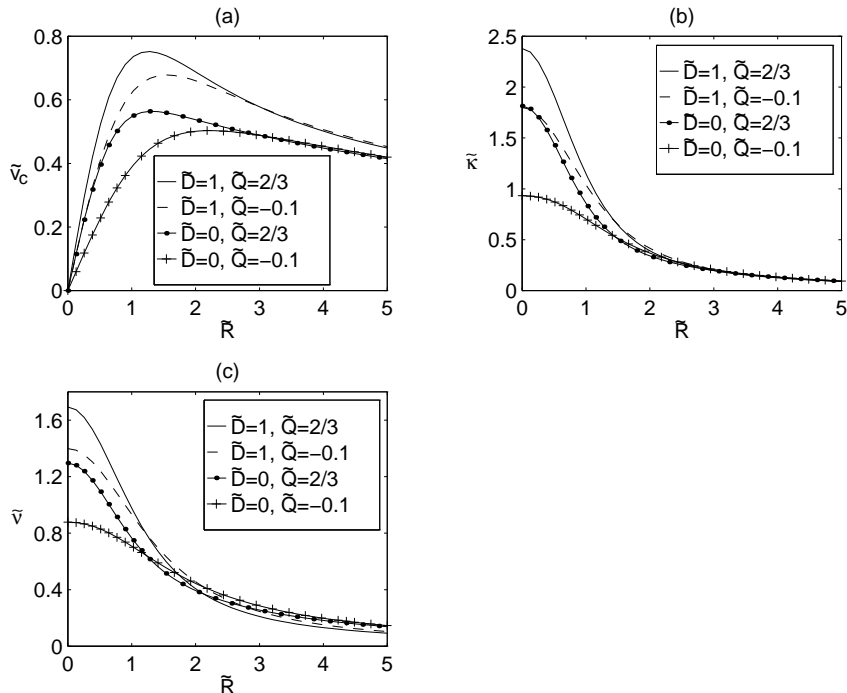


Figure 6: Curves of (a) the circular velocity \tilde{v}_c equation (12) in the galactic plane, (b) the epicyclic frequency $\tilde{\kappa}$ equation (13) and (c) the vertical frequency $\tilde{\nu}$ equation (14) for the same parameters as in figure 5.

Some level curves of the mass density, equation (11), are displayed in figures 5a–d. In general, as \tilde{D} and \tilde{Q} are lowered for a fixed \tilde{b} , the mass distribution profile becomes flatter. We also note from figures 6a–c that the maximum of the circular velocity is shifted to larger radii, and the epicyclic frequencies and vertical frequencies are lowered near the center.

2.3 Thin Disk Limit

To investigate the thin limit of the potential–density pairs deduced in the previous sections, it is more convenient to rederive an expression for the surface density, σ , by applying the transformation $z \rightarrow a + |z|$ on the multipolar expansion, equation (2) and using the well-known relation (Binney and Tremaine 1987),

$$\sigma = \frac{1}{2\pi G} \Phi_{,z}, \quad (15)$$

where the right-hand side is evaluated at $z \rightarrow 0^+$. We obtain

$$\tilde{\sigma} = \frac{1}{4\pi(\tilde{R}^2 + 1)^{7/2}} \left[2(\tilde{R}^2 + 1)^2(1 - \tilde{D}) + 6\tilde{D}(\tilde{R}^2 + 1) - 3\tilde{Q}(3\tilde{R}^2 - 2) \right]. \quad (16)$$

The variables and parameters were rescaled as in subsection 2.2, and $\sigma = m\tilde{\sigma}/a^2$. In particular cases with $\tilde{D} = 1$, $\tilde{Q} = 0$ and $\tilde{D} = 1$, $\tilde{Q} = 2/3$ we obtain Toomre's models 2 and 3, respectively (Toomre 1963). Expressions for the circular velocity and epicyclic frequency are given by equation (12) and equation (13) with $\tilde{b} = 0$, and the vertical frequency is calculated from equation (6) evaluated at $z \rightarrow 0^+$:

$$\tilde{\nu}^2 = \frac{1}{2(\tilde{R}^2 + 1)^{9/2}} \left[2\tilde{R}^6 + 9\tilde{R}^4(2\tilde{D} - \tilde{Q}) + 6\tilde{R}^2(-1 + \tilde{D} + 12\tilde{Q}) - 4(1 + 3\tilde{D} + 6\tilde{Q}) \right]. \quad (17)$$

Figure 7 shows curves of $\tilde{\sigma}_{,\tilde{R}} = 0$ (lines without circles) and $\tilde{\nu} = 0$ (lines with circles) as functions of \tilde{Q} and \tilde{R} for some values of the parameter \tilde{D} . In the thin limit, the disks always have regions of vertical instability. The Kuzmin disk ($\tilde{D} = \tilde{Q} = 0$) is stable for $\tilde{R} \geq \sqrt{2}$; Toomre's model 2 ($\tilde{D} = 1$, $\tilde{Q} = 0$) is stable for $\tilde{R} \geq \sqrt{2}\sqrt{-2 + \sqrt{6}}$; if $\tilde{Q} = 0$ the disk is stable for

$$\tilde{R} \geq \frac{\sqrt{2}}{2} \left[1 - 9\tilde{D} + \sqrt{3(27\tilde{D}^2 + 2\tilde{D} + 3)} \right]^{1/2} \quad (18)$$

if $\tilde{D} \geq -1/3$; and

$$0 \leq \tilde{R} \leq \frac{\sqrt{2}}{2} \left[1 - 9\tilde{D} - \sqrt{3(27\tilde{D}^2 + 2\tilde{D} + 3)} \right]^{1/2}, \quad (19)$$

$$\text{and } \tilde{R} \geq \frac{\sqrt{2}}{2} \left[1 - 9\tilde{D} + \sqrt{3(27\tilde{D}^2 + 2\tilde{D} + 3)} \right]^{1/2} \quad (20)$$

if $\tilde{D} < -1/3$.

In figure 8 we plot some curves of the surface density equation (16), the circular frequency equation (12) with $\tilde{b} = 0$, the epicyclic frequency equation (13) also with $\tilde{b} = 0$ and the vertical frequency equation (17) for some values of \tilde{D} and \tilde{Q} . The behaviour of the three first physical quantities, displayed as the multipole parameters are decreased, is very similar to those of the thick-disk model of the previous section.

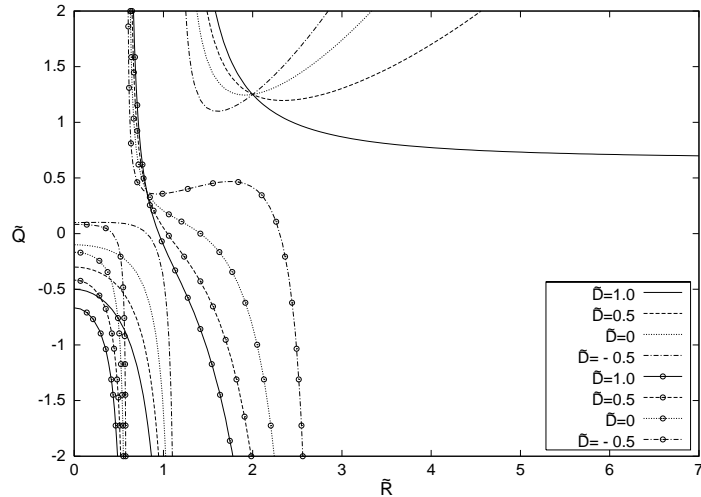


Figure 7: Curves of $\tilde{\sigma}_{\tilde{R}} = 0$ (lines without circles) and of $\tilde{\nu} = 0$ (lines with circles) as functions of \tilde{Q} and \tilde{R} for $\tilde{D} = 1, 0.5, 0, \text{ and } -0.5$.

3 Discussion

A Miyamoto and Nagai-like transformation was applied on the multipolar expansion up to the quadrupole term to produce potential–density pairs for flattened galaxies. These models, the first without the quadrupole term and the second with the quadrupole term, may be viewed as generalizations of the Miyamoto and Nagai models 2 and 3, respectively. The thin disk limit was also investigated and corresponds to generalizations of Toomre’s models 2 and 3. For each model we also calculated the velocity profile in the galactic plane and the epicyclic and vertical frequencies of oscillation of perturbed circular orbits.

The major drawback of our models is that the density distribution is not a monotone decreasing function of the radial and axial coordinates for arbitrary values of the free parameters. Thus we imposed the condition that the derivatives of the density distributions with respect to R and z do not have critical points, except at the origin. These imposed restrictions on the possible ranges of the multipole moments. We found that, except in the thin case limit, those restrictions were also sufficient to ensure non-negative circular velocities and also non-negative epicyclic and vertical frequencies (disk stability on the $z = 0$ plane).

D. Vogt thanks CAPES for financial support. P. S. Letelier thanks CNPq

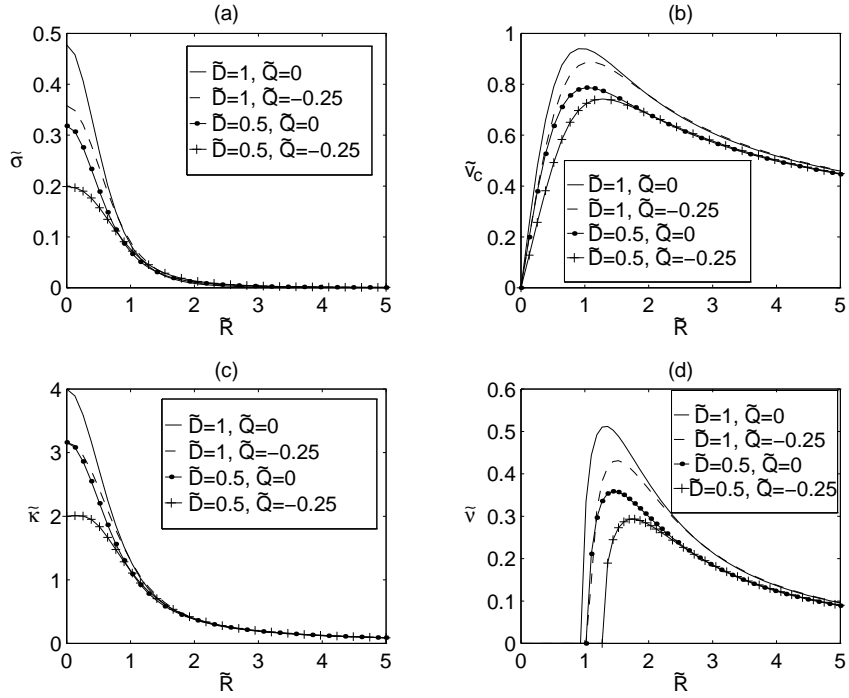


Figure 8: (a) Curves of the surface density equation (16), (b) the circular velocity equation (12) with $\tilde{b} = 0$, (c) the epicyclic frequency equation (13) with $\tilde{b} = 0$ and the vertical frequency equation (17). Parameters: $\tilde{D} = 1$, $\tilde{Q} = 0$ (solid lines); $\tilde{D} = 1$, $\tilde{Q} = -0.25$ (dashed lines); $\tilde{D} = 0.5$, $\tilde{Q} = 0$ (lines with points); $\tilde{D} = 0.5$, $\tilde{Q} = -0.25$ (lines with +).

and FAPESP for financial support. This research has made use of NASA's Astrophysics Data System.

References

- Bičák, J., Lynden-Bell, D., & Katz, J. 1993, *Phys. Rev. D*, 47, 4334
Binney, S., & Tremaine, S. 1987, *Galactic Dynamics* (Princeton, Princeton University Press), p. 121
de Zeeuw, T., & Pfenniger, D. 1988, *MNRAS*, 235, 949
González, G. A., & Letelier, P. S. 2000, *Phys. Rev. D*, 62, 064025
González, G. A., & Letelier, P. S. 2004, *Phys. Rev. D*, 69, 044013
Hernquist, L. 1990, *ApJ*, 356, 359
Jaffe, W. 1983, *MNRAS*, 202, 995
Lemos, J. P. S., & Letelier, P. S. 1994, *Phys. Rev. D*, 49, 5135
Long, K., & Murali, C. 1992, *ApJ*, 397, 44
Miyamoto, M., & Nagai, R. 1975, *PASJ* 27, 533
Morgan, L., & Morgan, T. 1970, *Phys. Rev. D*, 2, 2756
Morgan, T., & Morgan, L. 1969, *Phys. Rev.*, 183, 1097
Sato, C. 1980, *PASJ*, 32, 41
Toomre, A. 1963, *ApJ*, 138, 385
Vogt, D., & Letelier, P. S. 2003, *Phys. Rev. D*, 68, 084010
Vogt, D., & Letelier, P. S. 2005a, *Phys. Rev. D*, 71, 084030
Vogt, D., & Letelier, P. S. 2005b, *MNRAS*, 363, 268